Synthesis and properties of fluorene or carbazole-based and dicyanovinyl-capped n-type organic semiconductors†‡

Ting Qi,[ab] Yunqi Liu,*[a] Wenfeng Qiu,[a] Hengjun Zhang,[ab] Xike Gao,[ab] Ying Liu,[ab] Kun Lu,[ab] Chunyan Du,[ab] Gui Yu[a] and Daoben Zhu[a]

Received 15th October 2007, Accepted 3rd January 2008
First published as an Advance Article on the web 30th January 2008
DOI: 10.1039/b715920j

Dicyanovinyl-substituted compounds as electron transport materials are rarely studied, especially oligomers. A new series of fluorene or carbazole-based and dicyanovinyl-capped oligomers consisting of benzene or thiophene segments were synthesized using the Stille coupling reaction and their physical properties were investigated. Optical spectra show that the introduction of electron-accepting groups induces an intramolecular charge transfer, resulting in a shift of the absorption onset toward longer wavelengths. Moreover, the optical spectra of their films show intermolecular interactions, leading to bathochromic shifts with respect to the spectra in solution. Cyclic voltammetry indicates that they have suitable HOMO and LUMO energy levels, and the oligomers containing thiophene segments show lower LUMO levels. The X-ray crystallography of compound **FTCN** shows that the compound exhibits extended π stacking of the molecules. Thermal analysis reveals that they are thermally stable and no phase transition was observed at low temperatures.

1. Introduction

Organic semiconductors are intensively investigated from the viewpoints of their fundamental optoelectronic properties and their potential applications in organic field-effect transistors (OFETs),[1] organic light-emitting diodes,[2] and photovoltaic cells.[3] Most conjugated organic systems have inherently low electron affinities and therefore behave as p-type semiconductors and as hole-transport materials.[4] Recent advances in p-type organic semiconductors have fulfilled many of the requirements for use in diverse applications. However, n-type materials needed for complementary circuits present a challenge for chemists. New n-type organic semiconductors should have a suitable electron affinity larger than oxygen (1.46 eV),[5] excellent electron-transporting properties, and good solubility in organic solvents. The long-term exploration of this subject has shown the difficulty in fulfilling all of these desired properties simultaneously.[6]

One strategy to obtain air stable n-type organic semiconductors is modifying a conjugated core with strong electron-withdrawing substituents to lower its LUMO energy level so that the electron charge carriers are less susceptible to oxidation.[7] The most frequently used side groups so far are fluoro/fluoroalkyl[8] and cyano/dicyanomethylene[9] substituents. Dicyanomethylene-substituted quinoidal oligothiophene showed superior n-type characteristics.[9a,10] Recently, Takimiya and co-workers have synthesized highly soluble dicyanomethylene-substituted oligothiophenes with high electron mobilities (up to 0.16 $cm^2 V^{-1} s^{-1}$, $I_{on}/I_{off} \approx 1\times10^3$).[11] However, dicyanovinyl-substituted compounds as electron-transport materials are rarely studied,[12] especially oligomers. To date, Uhrich *et al.* have synthesized dicyanovinyl-substituted oligothiophenes reaching open circuit voltages of up to 1.04 V for solar cells (power conversion efficiencies of up to 1.6%).[12b] Here, we selected the dicyanovinyl group as the substituent because it has the following advantages: (i) the double bond can participate in the conjugation of the whole π-system and lead to efficient intermolecular interactions; (ii) the cyano groups have strong electron-accepting properties and may be useful for electron injection as suggested for a compound possessing pentafluorobenzene groups;[8c] (iii) the substituent can be easily introduced at the aromatic ring to control the HOMO–LUMO energy gap and the molecular packing. The fluorene and carbazole cores were chosen because they can increase the air stability of materials by lowering the HOMO energy level[13] and are suitable materials for OFETs.[14,15] Furthermore, the long alkyl chains can be easily introduced in the 9-position of the fluorene and carbazole rings, which may increase the solubility of the compounds and benefit the fabrication of devices. The hexyl side chain is optimum for charge transport due to its better self-organization.[1c,16]

In this paper, we report the synthesis and characterization of the dicyanovinyl-capped and fluorene or carbazole-based oligomers **FBCN**, **FTCN**, **CBCN** and **CTCN**. The introduction of benzene or thiophene rings is to extend π-conjugated systems. To the best of our knowledge, this series of compounds has not been reported. They would be promising electron transport materials as n-type organic semiconductors. The target compounds are characterized in detail, and their electronic properties are studied by UV-vis/fluorescence spectroscopy and cyclic voltammetry. The solid state structure of **FTCN** has been investigated (Fig. 1).

[a]*Beijing National Laboratory for Molecular Sciences, Organic Solids Laboratory, Institute of Chemistry, Chinese Academy of Sciences, Beijing 100080, China*
[b]*Graduate School of Chinese Academy of Sciences, Beijing 100080, China. E-mail: liuyq@mail.iccas.ac.cn*

† CCDC reference number 659317. For crystallographic data in CIF or other electronic format see DOI: 10.1039/b715920j

‡ Electronic supplementary information (ESI) available: X-Ray diffraction measurements, crystal structure and packing of **FTCN**, optical properties of **7** and **8** and electrochemical measurements for **FTCN**, **FBCN**, **CBCN**, CTCN, **7** and **8**. See DOI: 10.1039/b715920j

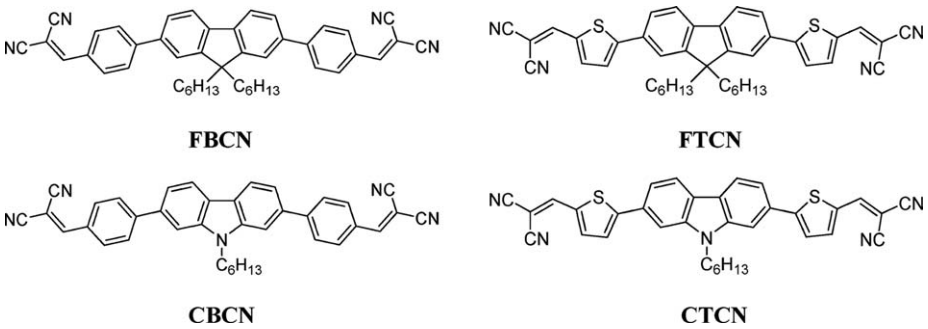

Fig. 1 Chemical structures of the target compounds.

2. Results and discussion

2.1. Synthesis and characterization

The target compounds **FBCN**, **FTCN**, **CBCN** and **CTCN** were synthesized *via* the Stille coupling reaction as illustrated in Scheme 1. Two types of cores of dialkylfluorene and alkylcarbazole were used. The alkyl substituents would increase the solubility of the target molecules in common organic solvents. 2,7-Dibromodialkylfluorene (**2**) was obtained by brominating with Br_2 solution directly from dialkylfluorene in high yield. 2,7-Dibromodialkylcarbazole (**6**) was prepared from alkylation of 2,7-dibromocarbazole (**5**) in high yield, and **5** was achieved by an efficient two-step synthesis according to the literature.[17] In this study, we use 2,7-dibromocarbazole because the 2,7-substituted carbazole is more favorable to the conjugation of the whole system relative to a 3,6-substituted one.[18] The synthetic methods for **3**[19] and **4**[20] were both reported in the literature under different reaction conditions. Here, we synthesized them under the same conditions *via* a Knoevenagel reaction.[21] In this reaction, malononitrile was condensed under Knoevenagel conditions (basic Al_2O_3 in dry toluene) with an aldehyde functionality to form the dicyanovinyl substituent. The corresponding compounds **3** and **4** were isolated in 71% and 72% yields. In the next step, dibromofluorene (**2**) and dibromocarbazole (**6**) were treated with *n*-BuLi and tri-*n*-butyltin chloride to afford the stannylated fluorene and carbazole. The organostannane was used directly in the next step without further purification. Stannylated fluorene reacted with 2 equiv. of compound **3** or **4** to afford the target products **FBCN** and **FTCN** in 51% and 53% yields, respectively. Similarly, stannylated carbazole was reacted with 2 equiv. of compound **3** or **4** to afford the target products **CBCN** and **CTCN** in 46% and 45% yields, respectively. As a general procedure, the reaction was performed using $PdCl_2(PPh_3)_2$ as a catalyst in toluene. For comparison, **7** and **8** were prepared under Suzuki cross-coupling conditions, and **7** has been reported in the literature.[22] Product **8** was isolated in reasonable yield (58%). The target molecules **FBCN** and **FTCN** are soluble in most common organic solvents, and the solubility of molecules **CBCN** and **CTCN** are moderate and inferior to **FBCN** and **FTCN**. Their structures were confirmed by ^{1}HNMR, ^{13}CNMR, EI-MS, and HRMS spectrometric methods.

2.2. Solid state structure of compound FTCN

The solubility of compound **FTCN** is the best in this series of target compounds, and it can form crystals very easily. We obtained red cuboid single crystals of **FTCN** by slow diffusion of 2 : 1 hexane–ethyl acetate. Unfortunately, the single crystals of other target compounds **FBCN**, **CBCN** and **CTCN** have not been obtained. An X-ray diffraction study was performed on the crystal of **FTCN** to determine its solid state structure (see ESI‡). As shown in Fig. 2, the molecular backbone is nearly planar (excluding the hexyl groups), and has a very slight twist along its long axis. The two dicyanovinyl end groups both deviated only 4° from the plane. The S atoms of thiophenes and the bridging carbon atom of the fluorene segment all face the same side. The two substituted alkyl chains are asymmetric. One is nearly perpendicular to the conjugate plane (~90°), and the other is reclined to 126° with respect to the plane.

Another peculiar structural feature of the compound concerns its molecular packing. The conjugate planes stack in an arrangement with a honeycomb, graphite structure (Fig. S3‡). For the fluorene–thiophene co-oligomers, such a kind of packing structure is rarely reported in the literature.[13b] The crystal structure is characterized by a "layer-by-layer" stacking mode viewed down the *b*-axis (Fig. 3), and the molecular arrangement is interdigitated and has parallel layers like a "bricklayer" structure. The unit cell contains four layers along the *c*-axis. Molecules pack in such a way that nearest neighbor molecules in the central two layers have the fluorene ring pointing in opposite directions. The mean distance between layers is 3.5 Å. The central two layers demonstrate a C–S short contact of 3.57 Å, and the side two layers demonstrate C–C short contacts of 3.39 Å and 3.55 Å. These data are indicated with dashed lines in Fig. 3. These distances are close to the van der Waals radii of sulfur–carbon (3.45–3.5 Å) and carbon–carbon (3.3–3.4 Å) atom pairs.[9b] These obviously indicate that π–π interactions exists between layers. However, due to the steric hindrance that the two asymmetric alkyl chains impose, the adjacent molecules between layers are interdigitated and oriented to form a ring (Fig. S2‡). Endless π–π stacking of the molecules' conjugated backbones results in infinite columns of porous structure with alkyl chains lying in the middle of rings (Fig. S3‡). This structure resembles a honeycomb graphite structure. Through packing of columns of rings, it extends the π stacking of the aromatic rings, leading to efficient electron transport in well-ordered thin films.

2.3. Optical properties

The electronic spectra of oligomers **FBCN**, **FTCN**, **CBCN** and **CTCN** were recorded in a CH_2Cl_2 solution and as thin films on quartz substrates (Table 1). **7** and **8** were studied under the

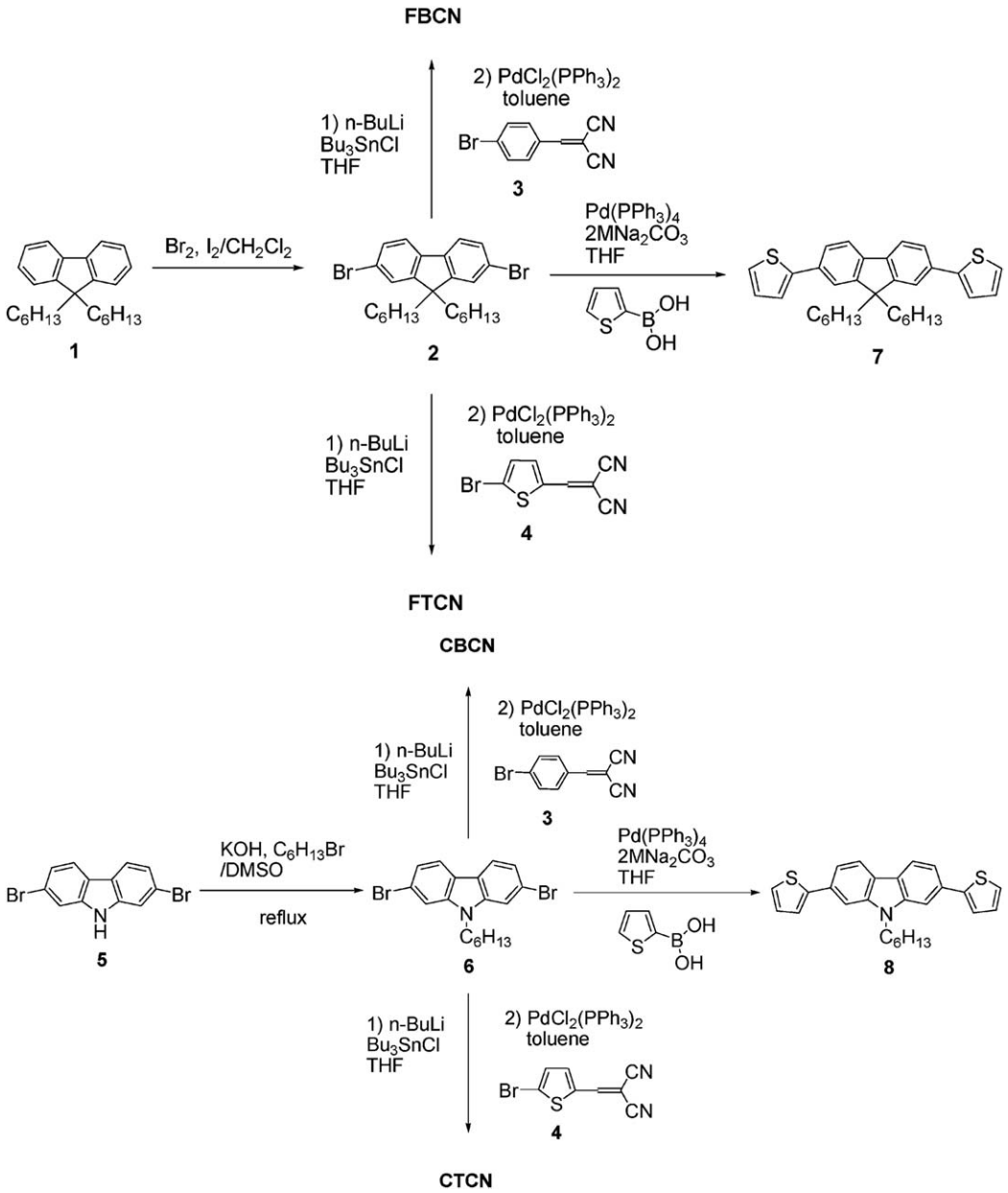

Scheme 1 Synthetic route to the target compounds.

same conditions to allow proper comparisons between dicyanovinyl-substituted and unsubstituted analogues.

The absorption spectra of the target compounds in solution exhibit three absorption bands, the absorption band at 289–308 nm is assigned to the π–π* transition (Fig. 4). Compared with **7** and **8**, respectively, **FTCN** and **CTCN** exhibit a large bathochromic shift (114 nm and 122 nm) of the absorption maximum (Fig. S4‡), which is attributed to the dicyanovinyl group taking part in the conjugation and the great stabilization of the LUMO by the electron-withdrawing groups.[23] Meanwhile, the introduction of electron-withdrawing groups produces the emergence of a new band at 400–550 nm assigned to an intramolecular charge transfer (ICT) between the aromatic ring donor part and the acceptor end groups.[24] The absorption bands of **FBCN** and **CBCN** are similar to those of **FTCN** and **CTCN**. The different cores (fluorene or carbazole) cannot bring obvious shifts of the absorption maxima in solution, but the introduction of different aromatic rings (thiophene or benzene) results in obvious bathochromic shifts. The compound containing thiophene segments **FTCN** (or **CTCN**) produces more than 50 nm bathochromic shift of the absorption maximum, much larger than one containing benzene segments **FBCN** (or **CBCN**). The results indicate that thiophene moieties enhance the charge transfer from the electron-rich moieties to electron-withdrawing groups. Their absorption spectra reveal similar trends in the solid state as shown in Fig. 5. Films were easily formed by spin coating from THF (1 mg ml^{-1}, quartz substrate). Optical band gaps (Table 1) in solution and solid state were approximated by extrapolation of the low-energy side of the absorption spectra to the baseline.[25] As expected, the energy

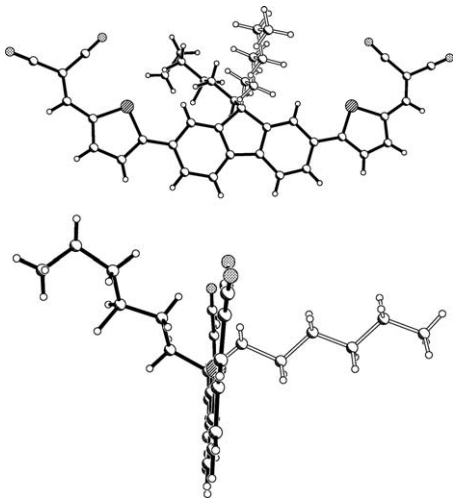

Fig. 2 Crystal structure of the molecule **FTCN**. (Top) top view. (Bottom) side view.

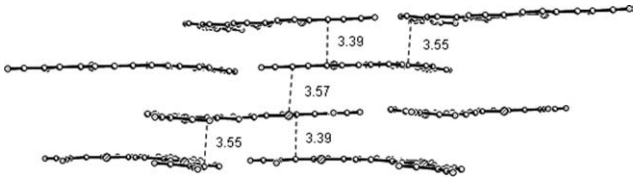

Fig. 3 View down the *b*-axis in crystals of **FTCN**, hydrogen atoms and alkyl groups are removed for clarity and all values are in angstroms.

band gaps of compounds decrease in the order, **7** > **8** > **FBCN** > **CBCN** > **FTCN** > **CTCN**, either in solution or in the solid state.

The fluorescence spectra of the target compounds in solution cover the visible spectrum from yellow to orange assigned to the $\pi_{Ar} \rightarrow \pi^*_{CV}$ ICT excited state.[24b] The phenomenon of bathochromic shifts of the emission maxima is not identical to the optical absorption. The emission maxima increase is in the order, **FBCN** < **FTCN** < **CBCN** < **CTCN** (Table 1), and the peak of **FTCN** almost overlaps with that of **CBCN**. Furthermore, the gradually increasing trend is more clearly observed in the solid state (Fig. 5). The emission spectrum of **FTCN** exhibits a blue shift relative to **CBCN** opposite to their absorption spectrum. This is clearly supported by the Stokes shifts between the fluorescence emission and the absorption maxima.

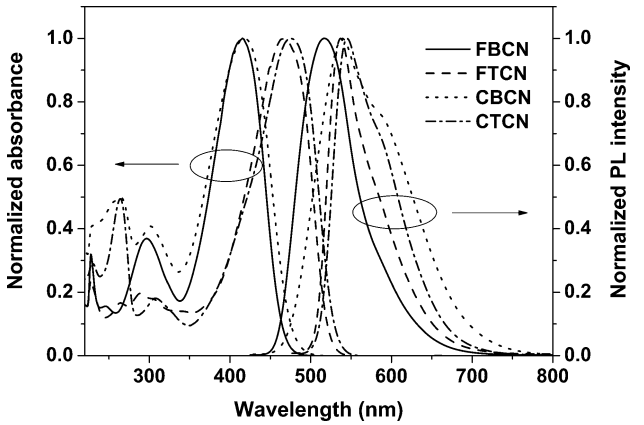

Fig. 4 Optical properties of the target compounds measured in CH_2Cl_2 solution.

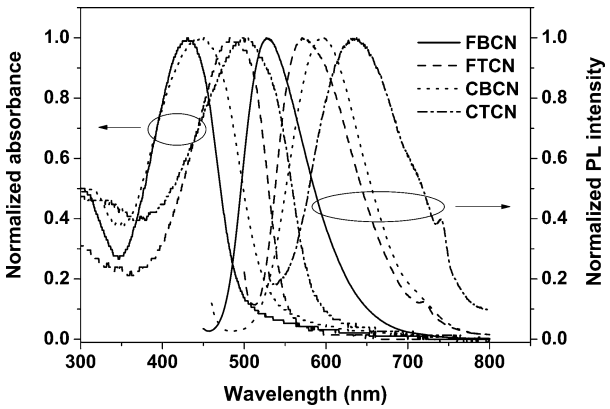

Fig. 5 Optical properties for films of the target compounds.

The Stokes shifts of the target compounds are relatively large, ranging from 70 to 121 nm in solution and from 88 to 148 nm in the solid state. In both states, **FTCN** has the smallest Stokes shift and **CBCN** has the largest one. The reason could be that the dipole moment of **CBCN** is larger than that of **FTCN**, and the emitting state of the former would be more stabilized by the ICT.[26] The fluorescence spectra of **7** and **8** in solution exhibit obvious blue shifts of the emission maxima with photoluminescence in the blue with respect to **FTCN** and **CTCN**, consistent with the absorption spectra (Fig. S4‡). The fluorescence spectra

Table 1 Optical data for compounds **FBCN**, **FTCN**, **CBCN**, **CTCN**, **7** and **8**

	Solution				Film[d]			
Compd	λ_{abs}[a]/nm (logϵ[a]/dm^3 mol^{-1} cm^{-1})	λ_{lum}[b] /nm	Stokes shift /nm	λ_{onset}[a]/nm (E_g[c]/eV)	λ_{abs}[e] /nm	λ_{lum}[b] /nm	Stokes shift /nm	λ_{onset} /nm (E_g[c]/eV)
FBCN	227, 296, 415(4.84)	517	102	467 (2.65)	430	527	97	502 (2.47)
FTCN	228, 289, 467(4.86)	537	70	526 (2.36)	483	571, 719	88	557 (2.23)
CBCN	264, 302, 418(4.79)	539	121	477 (2.60)	446	594	148	539 (2.30)
CTCN	264, 308, 475(4.86)	545	70	534 (2.32)	500	635, 741	135	595 (2.08)
7	229, 353(4.59)	386, 406	53	392 (3.16)	357	442, 467	85	404 (3.07)
8	270, 353(4.64)	394, 412	59	397 (3.12)	349	445, 470	96	407 (3.05)

[a] Measured in a dilute CH_2Cl_2 solution ($\sim 1 \times 10^{-5}$ M). [b] Excited at the absorption maxima. [c] Estimated from the onset of absorption ($E_g = 1240/\lambda_{onset}$). [d] Films were drop cast from THF (1 mg ml^{-1}, quartz substrate). [e] Reported values are the absorption maxima.

of **FTCN** and **CTCN** in the solid state present broader bandwidths with respective to those in solution.

From the solution to the solid state, the absorption and fluorescence spectra of the target compounds are red-shifted (see Table 1), due to the presence of stronger interactions between molecules (packing effect) in the solid state.[27] As shown in the single crystal structure (Fig. 3 and S3‡), **FTCN** has good π–π stacking in the solid state. The bathochromic shift of the UV-vis absorption observed in the solid state also can be explained by the crystal structure of **FTCN** that shows the J-aggregate conformation (Fig. 3). For the four target compounds, the bathochromic shifts of the absorption and emission maxima obviously show that the carbazole-based compounds shift to longer wavelengths relative to the fluorene-based compounds (Table 1). The difference in the molecular structure gives rise to the change in spectrum. The presence of two hexyl chains in the 9-position of the fluorene ring increases the intermolecular distances and thereby prevents better π stacking of the molecules,[28] which can be also confirmed by the crystal structure of **FTCN** (Fig. S2‡). The alkyl effect is reduced by the carbazole ring with one hexyl chain at the N atom, leading to stronger π stacking of the carbazole-based molecules.[27] When comparing dicyanovinyl-substituted compounds (**FTCN** and **CTCN**) with unsubstituted compounds (**7** and **8**), the absorption maxima of **7** and **8** are nearly invariant, but the introduction of dicyanovinyl groups strengthens intermolecular interactions in the solid state and results in the red-shift of the absorption maxima from the solution to solid state (Table 1).

2.4. Electrochemical properties

In order to investigate the electrochemical behaviors of oligomers **FBCN**, **FTCN**, **CBCN**, **CTCN**, **7** and **8**, cyclic voltammetry (CV) measurements were performed in CH_2Cl_2 containing 0.1 M n-Bu_4NPF_6 as a supporting electrolyte. The electrochemical potentials are summarized in Table 2. The CV of **FBCN**, **FTCN**, **CBCN** and **CTCN** displayed irreversible oxidative and reduction processes, while the CV of **7** and **8** only displayed irreversible oxidative processes under the same experimental conditions. Because of the introduction of the dicyanovinyl groups, the HOMO and LUMO energy levels of molecules are both lowered to a certain extent. Compared with unsubstituted compounds **7** and **8**, HOMO energy levels of **FTCN** and **CTCN** are stabilized by 0.27 eV and 0.28 eV, respectively. For the four target compounds, fluorene-based compounds display lower HOMO energy levels with respect to carbazole-based compounds. The HOMO energy level is mainly attributed to the contribution of the core (fluorene or carbazole) which leads to a stable energy level. The low HOMO levels may bring the target compounds good air stability. In the reduction processes, oligomers containing thiophene segments show lower LUMO energy levels with respect to ones containing benzene segments, indicating that thiophene segments shows larger contribution to n-type behavior. Electrochemical band gaps (Table 2) were calculated from the onset potentials of the anodic and cathodic processes and coincide with the calculated optical band gaps. Our results indicate that the target compounds would be ideal n-type materials.

Table 2 Electrochemical properties of π-conjugated compounds

Compd	E_{ox}[a] /V	E_{red}[a]/V	HOMO[b]/eV	LUMO[c]/eV	$\triangle E$[d]/eV	E_g^{opt}/eV
FBCN	1.76	−1.11	−6.00	−3.45	2.55	2.65
FTCN	1.64	−1.08, −1.64	−5.86	−3.56	2.30	2.36
CBCN	1.43	−1.21	−5.79	−3.46	2.33	2.60
CTCN	1.58	−1.08, −1.65	−5.78	−3.58	2.20	2.32
7	1.31	nd[e]	−5.63	nd[e]		
8	1.34	nd[e]	−5.50	nd[e]		

[a] Calculated from the potential at peak of oxidation and reduction. [b] Calculated using the empirical equation: HOMO = −(4.44 + E_{ox}^{onset}). [c] Calculated from LUMO = −(4.44 + E_{red}^{onset}). [d] Measured using a glassy carbon electrode as a working electrode, a platinum rod as a counter electrode, and Ag/Ag^+ as a reference electrode in CH_2Cl_2 containing 0.1 M n-Bu_4NPF_6 as a supporting electrolyte at a scan rate of 100 mV s^{-1} under an argon atmosphere. [e] Not determined.

2.5. Thermal properties

The thermal properties of the target compounds were evaluated by thermal gravimetric analysis (TGA) and differential scanning calorimetry (DSC). TGA revealed the onset decomposition temperatures of compounds **FBCN**, **FTCN**, **CBCN** and **CTCN** at 374 °C, 371 °C, 382 °C, and 372 °C, respectively. The results indicate their good thermal stability. As shown in Fig. 6, the heating and cooling DSC scans of the target compounds show no glass transitions up to 270–300 °C, due to the dense molecular packing.[29] Carbazole-based compounds **CBCN** and **CTCN** were both highly crystalline, exhibiting reversible thermal transitions and only a sharp melting point at 252 °C and 280 °C, respectively. In contrast, fluorene-based compounds behave totally differently. **FBCN** exhibited a sharp melting point at 216 °C lower than **CBCN** in the heating segment, and formed an amorphous state in the cooling segment. **FTCN** formed an amorphous state basically during the heating and cooling, and exhibited a broad and weak exothermic peak around 175 °C. These results further confirm the aforementioned alkyl effect where the molecules of carbazole-based compounds containing one hexyl chain are packed more tightly than those of fluorene-based compounds containing two hexyl chains. No phase transition

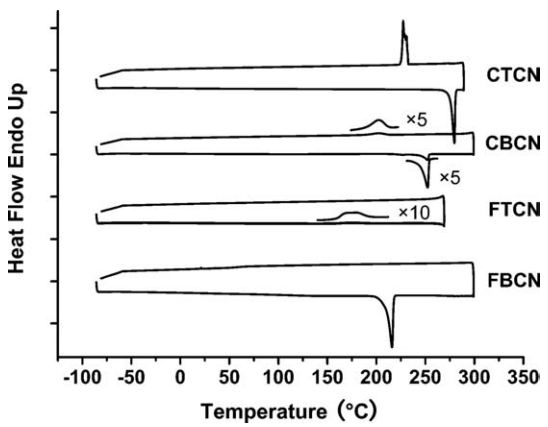

Fig. 6 DSC images of the target compounds with a heating and cooling rate of 10 °C min^{-1} under N_2.

at low temperatures indicates the series of compounds are highly desirable for application in devices.

3. Conclusions

A new series of fluorene or carbazole-based and dicyanovinyl-capped oligomers consisting of benzene or thiophene segments **FBCN**, **FTCN**, **CBCN** and **CTCN** have been synthesized and characterized. Optical spectra of these materials suggest that the introduction of electron-accepting groups induces an intramolecular charge transfer, resulting in a shift of the absorption onset towards longer wavelengths. Moreover, the optical spectra of their films show intermolecular interactions, leading to bathochromic shifts with respect to the spectra in solution. Coupled with thermal properties, the molecules of carbazole-based compounds are packed more tightly than those of fluorene-based compounds due to the alkyl effect. The crystal structure of **FTCN** also displays extended π stacking of molecules in the solid state. In addition, this class of materials shows suitable HOMO and LUMO energy levels, and the compounds attaching thiophene segments show lower LUMO energy levels. They also exhibited good thermal stability and no phase transition at low temperature. These behaviors make them promising candidates for n-channel semiconductors. Experiments are underway to test this hypothesis.

4. Experimental

4.1. General procedures

Chemicals were purchased from Aldrich, Alfa Aesar and used as received. Solvents and other common reagents were obtained from the Beijing Chemical Plant. THF and Toluene were dried and distilled immediately prior to use. ^{1}HNMR (400 MHz) and ^{13}CNMR (75 and 100 MHz) spectra were obtained on a Bruker DMX-300 and DMX-400 NMR Spectrometer using tetramethylsilane as the internal standard. High-resolution mass spectra (HRMS) and EI MS were both recorded on a Micromass GCT-MS spectrometer. Electronic absorption spectra were measured on a Jasco V570 UV-vis spectrophotometer. Emission spectra were recorded on a Hitachi F-4500 fluorescence spectrometer. TGA measurements were carried out on a TA SDT 2960 instrument under a dry nitrogen flow, heating from room temperature (RT) to 500 °C, with a heating rate of 10 °C min^{-1}. DSC analyses were performed on a TA DSC 2010 instrument under a dry N_2 flow, heating from −85 °C to 270–300 °C and cooling from 270–300 °C to −85 °C at a rate of 10 °C min^{-1}. Cyclic voltammetric measurements were carried out in a conventional three-electrode cell using Pt button working electrodes of 2 mm diameter, a platinum wire counter electrode, and a Ag/AgCl reference electrode on a computer-controlled CHI660C instruments at RT. X-Ray diffraction (XRD) measurements were carried out in the reflection mode at RT using a Rigaku MM-007 X-ray diffraction system (Mo Kα radiation, λ = 0.71073 Å). 9,9-Bis-*n*-hexylfluorene (**1**),[30] 2,7-dibromo-9,9-bis-*n*-hexylfluorene (**2**),[30] 2,7-dibromocarbazole (**5**),[17] 2,7-dibromo-9-(2-hexyl)carbazole (**6**),[15a] and 2,7-Bis(thiophene-2-yl)-9,9-bis-*n*-hexylfluorene (**7**)[22] were synthesized according to literature or slightly modified procedures.

4.2. Synthetic procedures

4.2.1. 4-Bromobenzylidenemalononitrile (3). 5-Bromothiophene-2-carboxaldehyde (1 g, 5.40 mmol), malononitrile (0.71 g, 10.80 mmol), and basic aluminum oxide (2.55 g) were stirred in toluene (50 ml) for 8 h at 70 °C. After cooling to room temperature, the reaction solution was diluted with toluene and filtered through a pad of silica gel, and the solvent of the filtrate was removed *in vacuo*. The crude product was purified by recrystallization from ethanol to give light yellow crystals **3** (889 mg, 71%): ^{1}HNMR (400 MHz, $CDCl_3$): δ (ppm) 7.78 (d, J = 8.62 Hz, 2 H), 7.71 (d, J = 6.48 Hz, 2 H), 7.68 (s, 1 H). ^{13}CNMR (100 MHz, $CDCl_3$): δ (ppm) 158.5, 133.2, 131.9, 130.0, 129.8, 113.6, 112.4, 83.6. EI-MS: m/z (%) = 232 (M^+, 100%).

4.2.2. 5-Bromo-2-dicyanovinylthiophene (4). This compound was prepared from 4-bromobenzaldehyde according to the procedure for **3** to give yellow crystals **4** in 72% yield: ^{1}HNMR (400 MHz, $CDCl_3$): δ (ppm) 7.74 (s, 1 H), 7.50 (d, J = 4.08 Hz, 1 H), 7.24 (d, J = 4.16 Hz, 1 H). ^{13}CNMR (100 MHz, $CDCl_3$): δ (ppm) 150.1, 138.9, 136.9, 132.1, 126.6, 113.6, 113.0, 78.7. EI-MS: m/z (%) = 240 (M^+, 100%).

4.2.3. General procedure for the Stille coupling reactions. 2.5 M *n*-BuLi (1.6 ml, 4.00 mmol) was added dropwise to a solution of **2** (or **6**) (885 mg, 1.80 mmol) in anhydrous THF (40 ml) at −78 °C under nitrogen with stirring. A deep pink precipitation was formed. After stirring for 1 h at −78 °C, tri-*n*-butyltin chloride (1.1 ml, 4.06 mmol) was added. The reaction mixture was then warmed to room temperature and stirred overnight. The clear solution was diluted with diethyl ether and washed with aqueous sodium bicarbonate solution (5%), and water. The organic layer was dried over $MgSO_4$, and the solvents were concentrated on a rotavap.

The above residue (1.48 g, 1.62 mmol), **3** (or **4**) (902 mg, 3.89 mmol), and $PdCl_2(PPh_3)_2$ (137 mg, 0.20 mmol) mixed in anhydrous toluene (40 ml) were heated at reflux under nitrogen for 36 h. The reaction mixture was allowed to cool to room temperature, poured into aqueous KF solution, and stirred at room temperature for 3 h. The resulting suspension was diluted with CH_2Cl_2 and filtered to remove polymeric tributyltin fluoride. The organic phase was separated, and the aqueous phase was extracted with CH_2Cl_2. The combined organic phase was washed with brine, dried with $MgSO_4$, and concentrated.

2,7-Bis[4-(1,1-dicyanovinyl)benzyl]-9,9-di-n-hexylfluorene (FBCN)

The crude product was separated by chromatography on silica gel (toluene) to give **FBCN** (527 mg, 51%). An analytical sample was purified by recrystallization from acetonitrile to give golden crystals: ^{1}HNMR (400 MHz, $CDCl_3$): δ (ppm) 8.04 (s, 2 H, CH=C(CN)$_2$), 8.02 (s, 2 H, Ph–H), 7.86–7.81 (m, 8 H, Ph–H), 7.69 (dd, J = 7.88 Hz, J = 1.54 Hz, 2 H, Ph–H), 7.63 (d, J = 1.30 Hz, 2 H, Ph–H), 2.09–2.00 (m, 4 H, CH_2), 1.13–1.01 (m, 12 H, CH_2), 0.75 (t, J = 6.96 Hz, 6 H, CH_3), 0.70–0.66 (m, 4 H, CH_2). ^{13}CNMR (75 MHz, $CDCl_3$): δ (ppm) 159.2, 152.4, 147.7, 141.4, 138.4, 131.6, 129.9, 128.2, 126.7, 121.7, 120.9, 114.1, 113.0, 82.0, 55.7, 40.4, 31.5, 29.7, 23.9, 22.6, 14.1. EI-MS: m/z (%) = 638 (M^+, 100%). HRMS (EI): calcd for $C_{45}H_{42}N_4$, 638.3409; found 638.3416.

2,7-Bis[5-(1,1-dicyanovinyl)thiophen-2-yl]-9,9-di-n-hexylfluorene (FTCN)

The crude product was separated by chromatography on silica gel (toluene) to give **FTCN** (558 mg, 53%). An analytical sample was purified by recrystallization from acetonitrile to give red crystals: ^{1}HNMR (400 MHz, $CDCl_3$): δ (ppm) 7.81 [s, 2 H, CH=C(CN)$_2$], 7.78 (s, 2 H, Ph–H), 7.76–7.72 (m, 4 H, Ph–H), 7.64 (d, J = 1.27 Hz, 2 H, Ar–H), 7.54 (d, J = 4.08 Hz, 2 H, Ar–H), 2.10–2.04 (m, 4 H, CH_2), 1.13–1.00 (m, 12 H, CH_2), 0.74 (t, J = 6.98 Hz, 6 H, CH_3), 0.65–0.61 (m, 4 H, CH_2). ^{13}CNMR (75 MHz, $CDCl_3$): δ (ppm) 157.4, 153.0, 151.0, 142.6, 140.7, 134.6, 132.2, 126.6, 125.2, 121.5, 121.2, 114.7, 113.9, 56.2, 40.6, 31.8, 29.9, 24.2, 22.9, 14.4. EI-MS: m/z (%) = 650 (M^+, 100%). HRMS (EI): calcd. for $C_{41}H_{38}N_4S_2$, 650.2538; found 650.2544.

2,7-Bis[4-(1,1-dicyanovinyl)benzyl]-9-(2-hexyl)carbazole (CBCN)

The crude product was separated by chromatography on silica gel (1 : 1 toluene–CH_2Cl_2) to give **CBCN** (414 mg, 46%). An analytical sample was purified by recrystallization from acetonitrile to give orange crystals: ^{1}HNMR (400 MHz, $CDCl_3$): δ (ppm) 8.23 [dd, J = 8.01 Hz, J = 4.16 Hz, 2 H, CH=C(CN)$_2$], 8.06 (d, J = 8.34 Hz, 4 H, Ph–H), 7.93–7.90 (m, 4 H, Ph–H), 7.81–7.72 (m, 2 H, Ph–H), 7.65–7.63 (m, 2 H), 7.56 (dd, J = 8.16 Hz, J = 0.78 Hz, 2 H, Ph–H), 4.47–4.41 (m, 2 H, CH_2), 2.00–1.93 (m, 2 H, CH_2), 1.46–1.27 (m, 6 H, CH_2), 0.89–0.85 (m, 3 H, CH_3). ^{13}CNMR (100 MHz, $CDCl_3$): δ (ppm) 159.2, 148.3, 141.9, 137.3, 131.6, 129.8, 128.5, 123.1, 121.5, 119.0, 114.1, 113.0, 107.7, 82.0, 43.4, 31.7, 29.2, 27.1, 22.7, 14.1. EI-MS: m/z (%) = 555 (M^+, 100%). HRMS (EI): calcd. for $C_{38}H_{29}N_5$, 555.2423; found 555.2431.

2,7-Bis[5-(1,1-dicyanovinyl)thiophen-2-yl]-9-(2-hexyl)carbazole (CTCN)

The crude product was separated by chromatography on silica gel (1 : 2 toluene–CH_2Cl_2) to give **CTCN** (413 mg, 45%). An analytical sample was purified by recrystallization from acetonitrile to give deep red crystals: ^{1}HNMR (400 MHz, $CDCl_3$): δ (ppm) 8.15 (d, J = 8.16 Hz, 2 H, CH=C(CN)$_2$), 7.83 (s, 2 H, Ph–H), 7.78 (d, J = 4.02 Hz, 2 H, Ph–H), 7.69 (s, 2 H, Ph–H), 7.62 (d, J = 8.11 Hz, 2 H, Ar–H), 7.58 (d, J = 4.06 Hz, 2 H, Ar–H), 4.42 (t, J = 7.09 Hz, 2 H, CH_2), 1.96–1.92 (m, 2 H, CH_2), 1.46–1.26 (m, 6 H, CH_2), 0.87 (t, J = 6.96 Hz, 3 H, CH_3). ^{13}CNMR (100 MHz, $CDCl_3$): δ (ppm) 157.5, 150.4, 141.7, 140.1, 134.3, 130.6, 124.8, 123.9, 121.6, 118.6, 114.2, 113.4, 107.0, 43.3, 31.5, 29.0, 26.9, 22.5, 13.9. EI-MS: m/z (%) = 567 (M^+, 100%). HRMS (EI): calcd for $C_{34}H_{25}N_5S_2$, 567.1551; found 567.1558.

2,7-Bis(thiophene-2-yl)-9-(2-hexyl)carbazole (8)

A mixture of **6** (1.21 g, 2.96 mmol), 2-thiopheneboronic acid (830 mg, 6.48 mmol), $Pd(PPh_3)_4$ (150 mg, 0.13 mmol), and 2 M Na_2CO_3 aqueous solution (13.6 ml, 27.20 mmol) in THF (40 ml) was stirred at reflux under a nitrogen atmosphere for 24 h. Water (150 ml) and CH_2Cl_2 (150 ml) were added. The organic phase was separated, washed with water, then brine solution, dried over anhydrous $MgSO_4$, filtered, and the solvents removed to dryness. The crude product was chromatographed on silica gel (4 : 1 petroleum–CH_2Cl_2) to give yellow solid **8** (712 mg, 58%). ^{1}HNMR (400 MHz, $CDCl_3$): δ (ppm) 8.05 (d, J = 8.08 Hz, 2 H), 7.59 (s, 2 H), 7.51 (d, J = 8.07 Hz, 2 H), 7.42 (d, J = 3.45 Hz, 2 H), 7.32 (d, J = 5.01 Hz, 2 H), 7.14 (dd, J = 4.83 Hz, J = 3.74 Hz, 2 H), 4.35 (t, J = 7.23 Hz, 2 H), 1.94–1.88 (m, 2 H), 1.48–1.28 (m, 6 H), 0.88 (t, J = 7.01 Hz. 3 H). ^{13}CNMR (100 MHz, $CDCl_3$): δ (ppm) 145.8, 141.6, 132.3, 128.2, 124.7, 123.2, 122.4, 120.8, 118.0, 106.1, 43.1, 31.7, 29.1, 27.1, 22.7, 14.2. EI-MS: m/z (%) = 415 (M^+, 100%). HRMS (EI): calcd. for $C_{26}H_{25}NS_2$, 415.1428; found 415.1430.

5. Acknowledgements

The present research was financially supported by the National Natural Science Foundation (20421101, 60671047, 50673093, 60736004), the Major State Basic Research Development Program (2006CB806203, 2006CB932103) and the Chinese Academy of Sciences.

6. References

1 (*a*) Y. Sun, Y. Liu and D. Zhu, *J. Mater. Chem.*, 2005, **15**, 53; (*b*) C. D. Dimitrakopoulos and P. R. L. Malenfant, *Adv. Mater.*, 2002, **14**, 99; (*c*) H. E. Katz, Z. Bao and S. L. Gilat, *Acc. Chem. Res.*, 2001, **34**, 359; (*d*) H. E. Katz, *J. Mater. Chem.*, 1997, **7**, 369; (*e*) K. Xiao, Y. Liu, T. Qi, W. Zhang, F. Wang, J. Gao, W. Qiu, Y. Ma, G. Cui, S. Chen, X. Zhan, G. Yu, J. Qin, W. Hu and D. Zhu, *J. Am. Chem. Soc.*, 2005, **127**, 13281; (*f*) Y. Wang, H. Wang, Y. Liu, C. Di, Y. Sun, W. Wu, G. Yu, D. Zhang and D. Zhu, *J. Am. Chem. Soc.*, 2006, **128**, 13058; (*g*) X. Gao, W. Wu, Y. Liu, S. Jiao, W. Qiu, G. Yu, L. Wang and D. Zhu, *J. Mater. Chem.*, 2007, **17**, 736–743.

2 (*a*) A. Kraft, A. C. Grimsdale and A. B. Holmes, *Angew. Chem., Int. Ed.*, 1998, **37**, 402; (*b*) U. Mitschke and P. Bäuerle, *J. Mater. Chem.*, 2000, **10**, 1471; (*c*) J. H. Burroughes, D. D. C. Bradley, A. R. Brown, R. N. Marks, K. Mackay, R. H. Friend, P. L. Burn and A. B. Holmes, *Nature*, 1990, **347**, 539.

3 (*a*) G. Yu, J. Gao, J. C. Hummelen, F. Wudl and A. J. Heeger, *Science*, 1995, **270**, 1789; (*b*) S. Roquet, A. Cravino, P. Leriche, O. Alévêque, P. Frère and J. Roncali, *J. Am. Chem. Soc.*, 2006, **128**, 3459; (*c*) A. Cravino, S. Roquet, P. Leriche, O. Alévêque, P. Frère and J. Roncali, *Chem. Commun.*, 2006, 1416.

4 M. Strukelj, F. Papadimitrakopoulos, T. M. Miller and L. J. Rothberg, *Science*, 1995, **267**, 1969.

5 L. M. Branscomb, *Nature*, 1958, **182**, 248.

6 (*a*) C. D. Dimitrakopoulos and D. J. Mascaro, *IBM J. Res. Dev.*, 2001, **45**, 11; (*b*) Z. Bao, *Adv. Mater.*, 2000, **12**, 227.

7 (*a*) C. R. Newman, C. D. Frisbie, D. A. da Silva Filho, J.-L. Brédas, P. C. Ewbank and K. R. Mann, *Chem. Mater.*, 2004, **16**, 4436; (*b*) X.-R. Zhang, W. Chao, Y.-T. Chuai, Y. Ma, R. Hao, D.-C. Zou, Y.-G. Wei and Y. Wang, *Org. Lett.*, 2006, **8**, 2563.

8 (*a*) Z. Bao, A. J. Lovinger and J. Brown, *J. Am. Chem. Soc.*, 1998, **120**, 207; (*b*) Y. Sakamoto, T. Suzuki, A. Miura, H. Fujikawa, S. Tokito and Y. Taga, *J. Am. Chem. Soc.*, 2000, **122**, 1832; (*c*) A. Facchetti, M.-H. Yoon, C. L. Stern, H. E. Katz and T. J. Marks, *Angew. Chem., Int. Ed.*, 2003, **42**, 3900; (*d*) J. F. Tannaci, M. Noji, J. McBee and T. D. Tilley, *J. Org. Chem.*, 2007, **72**, 5567; (*e*) A. Facchetti, J. Letizia, M.-H. Yoon, M. Mushrush, H. E. Katz and T. J. Marks, *Chem. Mater.*, 2004, **16**, 4715.

9 (*a*) T. M. Pappenfus, R. J. Chesterfield, C. D. Frisbie, K. R. Mann, J. Casado, J. D. Raff and L. L. Miller, *J. Am. Chem. Soc.*, 2002, **124**, 4184; (*b*) A. Yassar, F. Demanze, A. Jaafari, M. El Idrissi and C. Coupry, *Adv. Funct. Mater.*, 2002, **12**, 699; (*c*) T. M. Pappenfus, M. W. Burand, D. E. Janzen and K. R. Mann, *Org. Lett.*, 2003, **5**, 1535; (*d*) M. M. Bader, R. Custelcean and M. D. Ward, *Chem. Mater.*, 2003, **15**, 616.

10 (*a*) R. J. Chesterfield, C. R. Newman, T. M. Pappenfus, P. C. Ewbank, M. H. Haukaas, K. R. Mann, L. L. Miller and C. D. Frisbie, *Adv. Mater.*, 2003, **15**, 1278; (*b*) Y. Kunugi, K. Takimiya, Y. Toyoshima, K. Yamashita, Y. Aso and T. Otsubo, *J. Mater. Chem.*, 2004, **14**, 1367.

11 S. Handa, E. Miyazaki, K. Takimiya and Y. Kunugi, *J. Am. Chem. Soc.*, 2007, **129**, 11684.

12 (*a*) M. S. Liu, X. Jiang, S. Liu, P. Herguth and A. K.-Y. Jen, *Macromolecules*, 2002, **35**, 3532; (*b*) C. Uhrich, R. Schueppel, A. Petrich, M. Pfeiffer, K. Leo, E. Brier, P. Kilickiran and P. Baeuerle, *Adv. Funct. Mater.*, 2007, **17**, 2991.
13 (*a*) H. Meng, Z. Bao, A. J. Lovinger, B.-C. Wang and A. M. Mujsce, *J. Am. Chem. Soc.*, 2001, **123**, 9214; (*b*) M. Surin, P. Sonar, A. C. Grimsdale, K. Müllen, S. De Feyter, S. Habuchi, S. Sarzi, E. Braeken, A. Ver Heyen, M. Van der Auweraer, F. C. De Schryver, M. Cavallini, J.-F. Moulin, F. Biscarini, C. Femoni, R. Lazzaroni and P. Leclère, *J. Mater. Chem.*, 2007, **17**, 728.
14 (*a*) H. Meng, J. Zheng, A. J. Lovinger, B.-C. Wang, P. G. Van Patten and Z. Bao, *Chem. Mater.*, 2003, **15**, 1778; (*b*) B. M. Surin, P. Sonar, A. C. Grimsdale, K. Müllen, R. Lazzaroni and P. Leclère, *Adv. Funct. Mater.*, 2005, **15**, 1426; (*c*) M. C. Hamilton, S. Martin and J. Kanicki, *Chem. Mater.*, 2004, **16**, 4699; (*d*) E. Lim, B.-J. Jung, J. Lee, H.-K. Shim, J.-I. Lee, Y. S. Yang and L.-M. Do, *Macromolecules*, 2005, **38**, 4531.
15 (*a*) B. N. Drolet, J.-F. Morin, N. Leclerc, S. Wakim, Y. Tao and M. Leclerc, *Adv. Funct. Mater.*, 2005, **15**, 1671; (*b*) J.-F. Morin, N. Drolet, Y. Tao and M. Leclerc, *Chem. Mater.*, 2004, **16**, 4619.
16 (*a*) A. Babel and S. A. Jenekhe, *Synth. Met.*, 2005, **148**, 169; (*b*) Y. Zhu, A. Babel and S. A. Jenekhe, *Macromolecules*, 2005, **38**, 7983.
17 F. Dierschke, A. C. Grimsdale and K. Müllen, *Synthesis*, 2003, 2470.
18 (*a*) J.-F. Morin and M. Leclerc, *Macromolecules*, 2001, **34**, 4680; (*b*) J.-F. Morin and M. Leclerc, *Macromolecules*, 2002, **35**, 8413.
19 S. Wada and H. Suzuki, *Tetrahedron Lett.*, 2003, **44**, 399.
20 M.-M. M. Raposo, A.-M. C. Fonseca and G. Kirsch, *Tetrahedron*, 2004, **60**, 4071.
21 C.-L. Chiang, M.-F. Wu, D.-C. Dai, Y.-S. Wen, J.-K. Wang and C.-T. Chen, *Adv. Funct. Mater.*, 2005, **15**, 231.
22 V. Promarak and S. Ruchirawat, *Tetrahedron*, 2007, **63**, 1602.
23 J. Casado, T. M. Pappenfus, L. L. Miller, K. R. Mann, E. Orti, P. M. Viruela, R. Pou-Amérigo, V. Hernández and J. T. López Navarrete, *J. Am. Chem. Soc.*, 2003, **125**, 2524.
24 (*a*) H. Meier, *Angew. Chem., Int. Ed.*, 2005, **44**, 2482; (*b*) A. R. Katritzky, D.-W. Zhu and K. S. Schanze, *J. Phys. Chem.*, 1991, **95**, 5137.
25 J. Cao, J. W. Kampf and M. D. Curtis, *Chem. Mater.*, 2003, **15**, 404.
26 W. J. Yang, D. Y. Kim, M.-Y. Jeong, H. M. Kim, Y. K. Lee, X. Fang, S.-J. Jeon and B. R. Cho, *Chem.–Eur. J.*, 2005, **11**, 4191.
27 S. Tirapattur, M. Belletête, N. Drolet, M. Leclerc and G. Durocher, *Chem. Phys. Lett.*, 2003, **370**, 799.
28 S. Tirapattur, M. Belletête, N. Drolet, J. Bouchard, M. Ranger, M. Leclerc and G. Durocher, *J. Phys. Chem. B*, 2002, **106**, 8959.
29 S. Yao and K. D. Belfield, *J. Org. Chem.*, 2005, **70**, 5126.
30 S. H. Lee and T. Tsutsui, *Thin Solid Films*, 2000, **363**, 76.

